Electron electric-dipole-moment searches based on alkali-metal- or alkaline-earth-metal-bearing molecules

Edmund R. Meyer* and John L. Bohn
Department of Physics, JILA, NIST and University of Colorado, Boulder, Colorado 80309-0440, USA
(Received 23 July 2009; published 16 October 2009)

We introduce four new molecules—YbRb, YbCs, $YbSr^+$, and $YbBa^+$—that may prove fruitful in experimental searches for the electric-dipole moment (EDM) of the electron. These molecules can, in principle, be prepared at extremely low temperatures by photoassociating ultracold atoms and therefore may present an advantage over molecular-beam experiments. Here we discuss properties of these molecules and assess the effective electric fields they contribute to an electron EDM measurement.

DOI: 10.1103/PhysRevA.80.042508 PACS number(s): 33.15.−e, 31.15.A−, 11.30.Er

I. INTRODUCTION

It is by now widely acknowledged that experiments performed on atoms and molecules afford the best chance of measuring, or else limiting the possible size of, the electric-dipole moment (EDM) of the electron [1–3]. A lone valence electron inside an atom with large nuclear charge Z will feel an effective electric field enhanced beyond the field that is applied. For example, in atomic cesium, the apparent field is $132\mathcal{E}_{\mathrm{app}}$, where $\mathcal{E}_{\mathrm{app}}$ is the applied electric field [4]. This enhancement arises from the field's ability to mix the opposite-parity $6s$ and $6p$ states of Cs, and a fairly large applied electric field is still required. More recent estimates using *ab initio* methods give enhancement factors for Rb and Cs of 25.74 and 120.53, respectively [5]. Experiments on the Rb [6] and Cs [7] atoms are currently being pursued to take advantage of the enhancement factor and long hold times achievable in the alkali-metal-atom family.

Thus, to achieve effective electric fields of about 1–2 GV/cm, one would have to apply fields of $\sim 10-40$ MV/cm to these atoms. This is not desirable in practice. However, one can hold ultracold Rb and Cs atoms in traps for a time long compared to the typical molecular-beam experiment. Therefore, one applies a smaller electric field while taking advantage of the long coherence times. It is the tradeoff between hold time and effective electric field size that makes atomic electron EDM experiments attractive and worth pursuing.

Herein lies the rub: one wants a very large applied electric field, but with great electric fields come great systematic problems. It would therefore be beneficial if the s-p mixing could be achieved without the application of large laboratory electric fields. This is where molecules become interesting since they can be quite adept at mixing s- and p-atomic orbitals on their own, without the need for large applied electric fields. The field requirements to polarize the molecule may then be fairly modest. This important insight was initially due to Sandars and Lipworth [8].

Typically, experiments aimed at measuring the electron EDM in molecules have considered the simplest case of molecules with $^2\Sigma$ symmetry. Then there is only one unpaired electronic spin and it has zero orbital angular momentum about the internuclear axis. One appealing way to achieve fairly robust molecules for this purpose is to pair an atom in an s^2 configuration (such as Yb or Hg) with fluorine. Fluorine tends to capture an electron from any atom it encounters. Thus, when one of the s electrons is captured by F, a $^2\Sigma$ molecule is formed, as in YbF [1]. Moreover, the largely ionic bond is responsible for a large effective internal electric field that efficiently mixes the atomic s and p orbitals of the heavy atom [1,9].

In this paper, we suggest another class of $^2\Sigma$ molecules for EDM searches. Our emphasis is to consider molecules composed of atoms that can be laser cooled, thus, greatly reducing the molecular temperature well below that available in molecular-beam experiments. Specifically, we consider the neutral molecules YbRb and YbCs, along with the molecular ions $YbSr^+$ and $YbBa^+$. In all cases, laser cooling of the neutral atoms has been demonstrated [10–12]. Indeed, recently, short-lived ultracold samples of metastable $YbRb^\star$ have been produced via photoassociation [13]. This idea is very similar to the proposed van der Waals molecule CsXe [14].

These molecules, all of $^2\Sigma$ symmetry in their ground states, will have both advantages and disadvantages with respect to other molecules that are considered in EDM searches. The chief disadvantage is that their electronic wave function suggests a sharing, or covalency, of the bond and this somewhat limits the size of the effective electric field that they can sustain. We find that these fields are typically far smaller (10–100 times) than the leading contender ThO, with an $\mathcal{E}_{\mathrm{eff}}=104$ GV/cm [15]. Their main advantage is that they are cold enough to be trapped in either optical dipole traps or ion traps, leading conceivably to large coherence times within which to perform the experiment. In addition, these molecules, consisting of two heavy atoms, will have smaller rotational constants than the fluorides, hence, can be polarized in somewhat smaller fields. This is a feature that can help reduce systematic effects. Spin-rotational effects will also be reduced since they scale inversely with the reduced mass of the system; the electron remains fairly well decoupled from the molecular axis in the lower-lying rotational levels of the molecules. Another novel—though not necessarily beneficial—feature is that both atoms contain large-Z nuclei and thus can each contribute to the effective field.

*meyere@murphy.colorado.edu

In this paper, we therefore estimate the basic properties of these molecules, especially the effective electric fields they harbor. Section II will discuss the YbRb and YbCs molecules and give the details of the potential-energy surfaces and molecular parameters of the ground and excited states of interest. Section III will present the same information for the $YbSr^+$ and $YbBa^+$ molecular ions, as well as the neutrals from which they are derived. Section IV will detail the effective electric field calculations on the $^2\Sigma$ states of interest. Section V will present some concluding comments.

II. ALKALI-METAL–YTTERBIUM MOLECULES

Alkali-metal atoms, such as Rb and Cs, are the workhorses of laser cooling [16]. It is the unpaired *s* electron that is of interest in an electron EDM search since it is what we hope to coax into an *s*-*p*-hybridized atomic state. In the introduction, we discussed the role of fluorine, which can extract an electron from a closed *s*-shell atom such as Ba or Yb. We can accomplish the same feat by pairing an alkali-metal atom, such as Rb, with a closed *s*-shell atom, such as Yb, because Yb is more electronegative than any alkali-metal atom save H. This is similar to the pairing of Cs with Xe, as in [14], except Xe is a closed *p*-shell atom. Xe serves as a polarizing agent on the Cs atom, causing the Cs *s* and *p* orbitals to hybridize. Moreover, the difference in electronegativity is greater between Cs and Yb than between Rb and Yb, so that the YbCs molecule might be expected to be the more polar of the two. However, it is also important to consider the bonding length. A larger bond length would work to counteract the charge-transfer mechanism because the two atoms would not get close enough together to allow the atomic wave functions to overlap. In order to understand the true details, we turn to *ab initio* methods in order to gain understanding into the nature of the bonding process.

For the YbRb and YbCs systems, we use the MOLPRO suite of codes [17]. We start at an interatomic distance $R=25a_0$ and move in to $R=4.8a_0$. At $R=25a_0$, we perform a self-consistent field Hartree-Fock (SCF-HF) calculation on the closed-shell Yb–alkali-metal molecular ion system to obtain a starting wave function. We then perform a second SCF-HF on the neutral YbRb molecule followed by a multiconfiguration self-consistent field calculation (MCSCF) [18,19]. The MCSCF contains the ground $X\ ^2\Sigma$ as well as the excited $a\ ^2\Pi$ and $b\ ^2\Sigma$ states arising from the alkali-metal *np* configurations. This is the starting configuration for the multireference configuration-interaction (MRCI) [20,21] calculation performed in each molecular symmetry group. We use an active space of {6,3,3,0} with no closed orbitals. We used the Stuttgart basis sets and effective core potentials (ECPs) with core-polarization potentials (CPP) for the alkali-metal atom and Yb. We used the ECP68MDF potential [22] for Yb, ECP36SDF potential for Rb [23,24], and ECP54SDF potential for Cs [23]. All of the basis sets associated with the ECPs were left uncontracted. The active spaces in the calculations were chosen such that the experimental excitation energy of the alkali-metal atom was reproduced to within 50 cm^{-1}.

The results of the potential calculations are presented in Figs. 1(a) and 1(b), for the ground state and the two lowest-lying dipole-allowed excited states in Hund's coupling case (a). The inset is an enlargement of the ground state showing that, while far shallower than alkali-metal dimer potentials, it is expected to hold bound states. Table I gives the relevant molecular parameters such as bond length, vibrational constant, dissociation energy, and rotation constant. The parameters were obtained by fitting the *ab initio* points to a Morse potential. Both YbCs and YbRb exhibit a large bonding length greater than $10a_0$ in the ground $X\ ^2\Sigma$ state. Due to the very shallow potential and large bond length, these molecules appear to be of a van der Waals-type bonding nature, similar to that found in CsXe [14].

In each figure, the solid arrow denotes the photoassociation step needed to drive the initial atom pair into an excited-state molecule. For YbRb, this step has already been demonstrated experimentally [13]. Also shown schematically as a dashed arrow is the transition necessary to create molecules in the ground electronic, vibrational, and rotational states. Depending on which levels can ultimately be accessed in the first photoassociation step, this second transition may not be possible in a single step. The quest to produce ultracold ground-state polar molecules from ultracold atoms is currently a major research area, which has recently seen the production of molecular ground states [25–27].

The *ab initio* calculations show that while the dominant contribution to the unpaired electron is from the Rb 5*s* (Cs 6*s*) orbital, there are appreciable contributions from the Rb 5*p* (Cs 6*p*) as well as the Yb 6*s* and 6*p* atomic configurations. A secondary contribution comes from a similar arrangement except that the Yb 6*p* atomic orbital has a more

TABLE I. Molecular parameters for YbRb and YbCs. Bond distance r_e, dissociation energy (D), vibration constants (ω_e and $\omega_e\chi_e$), rotation constants (B_e and D_e), and vibration-rotation mixing constants α_e. r_e is in atomic units, while all others are in cm^{-1}.

Molecule	r_e	D	ω_e	$\omega_e\chi_e$	B_e (10^{-2})	D_e (10^{-9})	α_e (10^{-4})
YbRb $X\ ^2\Sigma$	10.22	194	12.6	0.21	0.99	24	1.65
YbRb $a\ ^2\Pi$	7.44	3380	66.4	0.33	1.86	5.9	1.00
YbRb $b\ ^2\Sigma$	8.52	942	36.0	0.34	1.42	8.8	1.32
YbCs $X\ ^2\Sigma$	10.69	182	9.9	0.13	0.69	14	0.99
YbCs $a\ ^2\Pi$	7.91	2710	50.9	0.24	1.27	3.2	0.63
YbCs $b\ ^2\Sigma$	9.41	490	20.9	0.22	0.90	6.6	092

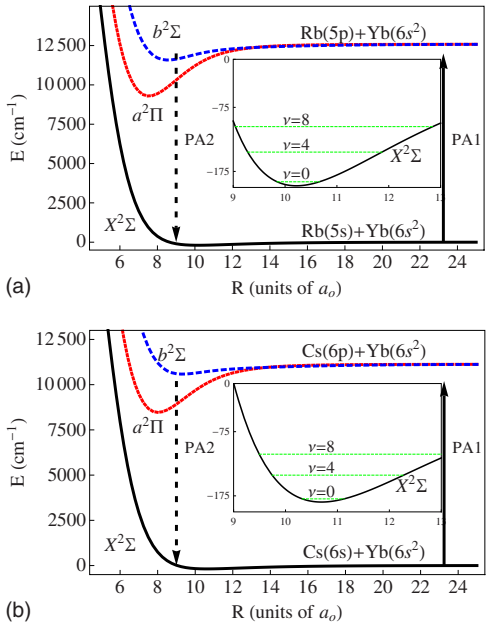

FIG. 1. (Color online) Potential-energy surfaces for the YbRb (a) and YbCs (b) molecules. a_0 is the Bohr length and is 0.529 18 Å. The ground- to excited-state energy splitting in the separated limit was optimized to produce the Rb (Cs) $5(6)s \rightarrow 5(6)p$ transition known experimentally. The arrows indicate the two-color photoassociation route to producing ultracold polar molecules in the ground $X\ ^2\Sigma$ state. The inset shows the $\nu=0,4,8$ vibrational levels of the ground electronic state.

pronounced presence in the second σ-molecular orbital. There is some, albeit little, charge transfer from the alkali-metal atom to Yb. At the potential minima, Rb transfers more charge to Yb than does Cs, counter to what is expected based on electronegativity arguments. However, this can be understood in terms of the bond length in YbCs being larger than in YbRb. The excited $a\ ^2\Pi$ state of both YbRb and YbCs contains a far shorter bond length as well as a deeper well than the ground $X\ ^2\Sigma$ state. This is due to the larger polarizability in the $5(6)p$ state of Rb (Cs).

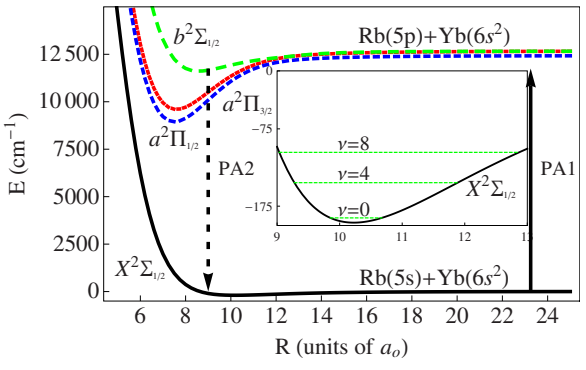

FIG. 2. (Color online) YbRb potential-energy curves with spin-orbit effects included. a_0 is the Bohr length, 0.529 18 Å. The effective core potential ECP36SDF was modified to produce the $5p\ ^2P_{1/2} \rightarrow 5p\ ^2P_{3/2}$ energy splitting of Rb. The arrows indicate the two-color photoassociation route. The inset shows the vibrational levels $\nu=0,4,8$ of the ground electronic state of interest.

In order to obtain a higher level of accuracy in describing the excited $a\ ^2\Pi$ state, we included the effects of spin-orbit coupling in the *ab initio* calculations. We then modified our long-range potential to match the experimentally determined C_6 coefficient determined by [13]. Figure 2 gives the potentials with spin-orbit terms applied throughout. The spin-orbit terms of the ECP36SDF effective core potential of the Stuttgart group were modified so as to reproduce the $5p\ ^2P_{1/2} \rightarrow 5p\ ^2P_{3/2}$ energy splitting of the Rb atom to within a few cm^{-1}. The $X\ ^2\Sigma_{1/2}$ state is fairly unaffected by the presence of the spin-orbit terms; this is due to the large electronic energy separation of the ground and excited electronic states compared to the atomic spin-orbit constant in the alkali-metal atoms. There are now three excited states since the $^2\Pi$ state splits into two surfaces, one each for where the electronic spin lies parallel or antiparallel to the electronic orbital angular momentum. In addition, at large separations of about $11a_o$, there is an avoided crossing between the $a\ ^2\Pi_{1/2}$ and the $b\ ^2\Sigma_{1/2}$ states due to the spin-orbit interaction. This changes the outer wall behavior of both states.

We again fit the *ab initio* points to a Morse potential in order to obtain the spectroscopic parameters describing the states of interest (see Table II). There is very little change in the parameters for the $X\ ^2\Sigma_{1/2}$ state. The excited $a\ ^2\Pi_{1/2}$ state has a slightly smaller bond length but larger well depth, while the $a\ ^2\Pi_{3/2}$ state has a longer bond length and smaller well depth compared to the $a\ ^2\Pi$ state in the previous calculation.

III. ALKALINE-EARTH-METAL–YTTERBIUM MOLECULAR IONS

In addition to the neutral molecules considered in the previous section, we can also consider their isoelectronic cation partners $YbSr^+$ and $YbBa^+$. The molecules might be expected to form deeper wells and shorter bond lengths because the atomic cations Sr and Ba will strongly attract an electron. Also, these ions offer intriguing possibilities for an EDM experiment in a stable ion trap, as has been recently proposed [28]. Another possibility is to arrange the molecular ions into an optical lattice. In addition, replacing the alkali-metal atoms with alkaline-earth metals affords the possibility of isotopomers with zero nuclear spin on both atoms, thus, greatly simplifying their spectroscopy.

We performed a SCF-HF followed by an MCSCF [18,19] calculation on the neutral and ionic species of the alkaline-earth-metal-atom–Yb separated atoms. Once again the Stuttgart basis set and ECPs ECP68MDF were used to describe the Yb [22] atom, while the ECP36SDF and ECP54SDF [24] basis set and ECP were used to describe the Sr and Ba atoms, respectively. CPPs were included as well. In the neutral molecule, we accounted for the $X\ ^1\Sigma$, $A\ ^3\Pi$, $B\ ^3\Sigma$, $a\ ^1\Pi$, and $b\ ^1\Sigma$ electronic states. In the ionic state, we kept the three lowest $^2\Sigma$ states and the $^2\Pi$ state. The final step in the calculations involved performing an MRCI [20,21] calculation on each spin multiplicity and group symmetry. The potential-energy surfaces are presented in Figs. 3(a) and 3(b). The upper (lower) set of curves in each panel are the ionic (neutral) molecules.

TABLE II. Molecular parameters for YbRb including spin-orbital effects. Bond distance r_e, dissociation energy (D), vibration constants (ω_e and $\omega_e\chi_e$), rotation constants (B_e and D_e), and vibration-rotation mixing constant α_e are all determined from the Morse potential parameter. r_e is in atomic units, while all others are in cm^{-1}.

Molecule	r_e	D	ω_e	$\omega_e\chi_e$	B_e (10^{-2})	D_e (10^{-9})	α_e (10^{-4})
YbRb $X\ ^2\Sigma_{1/2}$	10.23	193	12.4	0.20	0.99	25	1.64
YbRb $a\ ^2\Pi_{1/2}$	7.39	3590	70.9	0.35	1.89	5.4	1.00
YbRb $a\ ^2\Pi_{3/2}$	7.52	3120	65.4	0.34	1.83	5.7	1.02
YbRb $b\ ^2\Sigma_{1/2}$	8.58	1026	33.9	0.28	1.40	9.6	1.20

A possible route to make the molecular ions is presented in Figs. 3(a) and 3(b). By driving near the alkaline-metal-earth-atom $^1S \rightarrow {}^1P$ transition, one can photoassociate molecules into a high-lying vibrational level of the $^1\Pi$ (or $^1\Sigma$) state (solid arrow). From this state, a photoionization pulse to the $X\ ^2\Sigma$ state of the molecular ion should produce molecules in the electronic state of interest for an electron EDM experiment [long dashed potential in the upper portion of each panel in Figs. 3(a) and 3(b)].

A typical Ramsey experiment would measure the energy difference between two levels with differing angular momentum projections M_s referred to a laboratory magnetic field. The measurement consists of the time-varying population of one of these states. To measure this, one could drive the molecule to the purely repulsive $a\ ^2\Sigma$ state (short dashed arrow), which dissociates into the Sr (Ba) $5(6)s^2$ and Yb^+ $6s$ atomic states. If the dissociation laser were polarized to drive only one M_s state, then efficient detection of the Yb^+ ions serves as a high signal-to-noise detection.

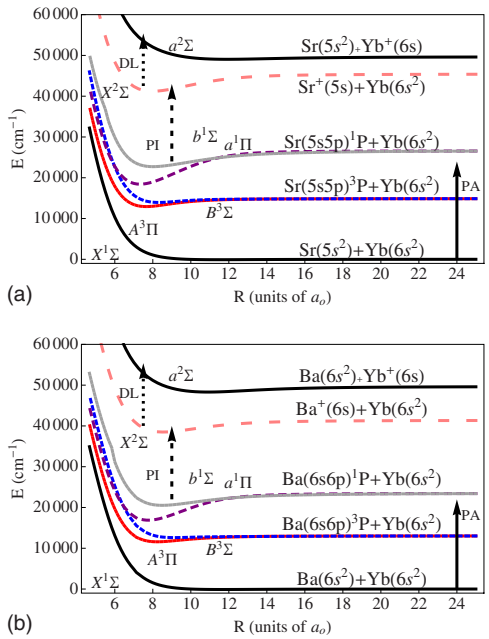

FIG. 3. (Color online) Potential-energy surfaces for the YbSr (a) and YbBa (b) molecules in their neutral (lower set of curves) and ionic (upper set of curves) states. a_0 is the Bohr length, 0.529 18 Å. The ground neutral state to the ground ionic state energy splitting in the separated limit was optimized to produce the ionization levels known experimentally. The arrows indicate the photoassociation (solid arrow), photoionization (medium dashed arrow), and proposed dissociation pulse (short dashed arrow) in the electron EDM search.

These potential-energy surfaces of the alkaline-earth-metal-atom–Yb ionic molecules are markedly different from the neutral species alkali-metal-atom–Yb systems. First, the bond distance is reduced to around $8a_0$ and the well depth increased by an order of magnitude. Physically, this is easy to understand. The Sr and Ba ions (in the separated limit) are very willing to accept an electron; hence, they have a tendency to take an electron from the neutral Yb atom. Thus, charge is efficiently transferred from the Yb atom to the alkaline-earth-metal ion and an ionic-type bond is formed, as compared to the more shallow van der Waals-type bond in YbRb and YbCs. This circumstance is also responsible for the larger body-fixed molecular electric-dipole moment that in the neutrals.

The second surface in the ion is the $a\ ^2\Sigma$ state, which is repulsive above the equilibrium bond length of the $X\ ^2\Sigma$. The excited-state surface in $YbBa^+$ is deeper than $YbSr^+$; however, the dissociation laser should still be able to drive the ground state to an unbound state of the system due to the rather large bond length of the $a\ ^2\Sigma$ state in the molecular ions. The excited $a\ ^2\Sigma$ state is more closely akin to the ungerade states of homonuclear molecules. In this instance, at the bond length of the $X\ ^2\Sigma$ molecule, the configuration is a combination of two molecular orbitals: one of Ba($6s^1$)-Yb($6s^2$) and the other of Ba($6s^2$)-Yb($6s^1$) hybridized atomic configurations. The excited state is the orthogonal combination. Whereas the ground state has an electronic distribution favorable to a deep bond the excited state does not.

Table III gives the molecular parameters for a few states of interest in the YbSr and YbBa systems. Once again, we fit the tabulated points from the *ab initio* calculations to a Morse potential. The neutral molecules contain very shallow wells. This is attributed to each atom influencing the other and causing a slight mixing of atomic s and p orbitals. This is a van der Waals interaction, which creates the ground neutral molecular states. However, the molecular ion states are created by having an electron from Yb have significant amplitude at the site of the alkaline-earth-metal atom. There is expected to be significant mixing of atomic s and p orbitals on both atoms.

TABLE III. Molecular parameters for YbSr and YbBa. Bond distance r_e, dissociation energy (D), vibration constants (ω_e and $\omega_e\chi_e$), rotation constants (B_e and D_e), and vibration-rotation mixing constant α_e are all determined from the Morse potential parameter. r_e is in atomic units, while all others are in cm^{-1}.

Molecule	r_e	D	ω_e	$\omega_e\chi_e$	B_e (10^{-2})	D_e (10^{-9})	α_e (10^{-4})
YbSr $X\ ^1\Sigma$	11.42	94	8.6	0.19	0.78	26	1.72
YbSr $a\ ^1\Pi$	7.30	8460	94.0	0.26	1.98	3.2	0.63
$YbSr^+$ $X\ ^2\Sigma$	7.94	4230	61.5	0.22	1.62	4.5	0.70
YbBa $X\ ^1\Sigma$	11.64	112	7.86	0.14	0.57	12	0.98
YbBa $a\ ^1\Pi$	7.67	6765	73.4	0.20	1.32	1.7	0.41
$YbBa^+$ $X\ ^2\Sigma$	8.50	2810	42.8	0.16	1.08	2.7	0.47

IV. EFFECTIVE ELECTRIC FIELD CALCULATION

The effective electric field is defined by the energy shift incurred by the EDM Hamiltonian $H_{\mathrm{EDM}}=-\vec{d}_{\mathrm{e}}\cdot\vec{\mathcal{E}}_{\mathrm{eff}}$ acting on a putative electric-dipole moment d_{e}. We have previously detailed a perturbative method for estimating $\mathcal{E}_{\mathrm{eff}}$ to within $\sim 25\%$ based on our nonrelativistic molecular orbitals [15,29], following the work in [4]. The basic idea is that we can separate the calculation into an analytic and numeric piece via (in atomic units)

$$\mathcal{E}_{\mathrm{eff}}=\frac{\langle\Psi_{\mathrm{mol}}|H_{\mathrm{EDM}}|\Psi_{\mathrm{mol}}\rangle}{-d_{\mathrm{e}}}=\frac{4\sigma}{\sqrt{3}}\epsilon_s\epsilon_p\Gamma_{\mathrm{rel}}Z, \tag{1}$$

where Γ_{rel} is a relativistic factor that depends on the atomic properties and is given by an analytic expression. $\sigma=1/2$ is the electron projection on the molecular axis. Z is the number of protons in the heavy atom. The values of ϵ_s and ϵ_p represent the amount of s- and p-atomic orbitals contained in the relevant molecular orbital and are obtained from nonrelativistic electronic structure calculations.

The estimate in the cases studied in [15,29] was for systems with one heavy atom and one light atom. Therefore, the dominant contribution to $\mathcal{E}_{\mathrm{eff}}$ arises from the heavy atom. This is because the relativistic factor Γ_{rel} scales as Z^2; thus, the effective electric field $\mathcal{E}_{\mathrm{eff}}$ scales as Z^3. In the examples we are considering here, both atoms contribute since they have similar Z. Therefore, it should be expected that the electron experiences an average effective electric field from both atoms. What remains to be determined is whether the atoms are polarized parallel or antiparallel to each other; this will be addressed below.

Since Γ_{rel} depends on the atomic properties of the atom considered, we break the two contributions up by expanding our molecular wave function as follows:

$$|\Psi_{\mathrm{mol}}\rangle=\epsilon_{\mathrm{s,A}}|As\rangle+\epsilon_{\mathrm{p,A}}|Ap\rangle+\epsilon_{\mathrm{s,Yb}}|\mathrm{Yb}s\rangle+\epsilon_{\mathrm{p,Yb}}|\mathrm{Yb}p\rangle, \tag{2}$$

and verified the condition $\langle\Psi_{\mathrm{mol}}|\Psi_{\mathrm{mol}}\rangle=1$ at all times in the calculation. The subscript A refers to either an alkali-metal or alkaline-earth-metal atom. With this wave function, we can calculate the quantity $\mathcal{E}_{\mathrm{eff}}$ via

$$\mathcal{E}_{\mathrm{eff}}=\frac{\langle\Psi_{\mathrm{mol}}|H_{\mathrm{EDM}}|\Psi_{\mathrm{mol}}\rangle}{-d_{\mathrm{e}}}=\mathcal{E}_{\mathrm{eff,A}}+\mathcal{E}_{\mathrm{eff,Yb}}. \tag{3}$$

The only surviving terms are $\langle A,s|H_{\mathrm{EDM}}|A,p\rangle$ and $\langle\mathrm{Yb},s|H_{\mathrm{EDM}}|\mathrm{Yb},p\rangle$ and so the contributions from each atom simply add. The terms are individually calculated via the methods described in [15,29]. Now, if the product $\epsilon_{\mathrm{s,A}}\epsilon_{\mathrm{p,A}}$ is of the same (opposite) sign as $\epsilon_{\mathrm{s,Yb}}\epsilon_{\mathrm{p,Yb}}$ then the individual effective electric fields $\mathcal{E}_{\mathrm{eff,A}}$ and $\mathcal{E}_{\mathrm{eff,Yb}}$ would add (subtract). Since each term has an uncertainty of 25% associated with it and because these errors are not completely random, we report that these current estimates are 50% certain.

One thing we discover in the *ab initio* calculations is that there are two large contributions to the overall molecular orbital, as discussed in Sec. II. In the alkali-metal atoms, this mixing of molecular configurations is more pronounced than in the alkaline-earth-metal atoms. These configurations are different zero angular momentum projections of atomic orbitals from each atom. We find that these two configurations are $|\Psi_1\rangle=|\sigma_2^1\sigma_3^0\rangle$ and $|\Psi_2\rangle=|\sigma_2^0\sigma_3^1\rangle$ for two different molecular orbitals σ_2 and σ_3.

In the case of YbRb and YbCs σ_2 is primarily a Rb(Cs)5s (6s) atomic orbital with appreciable mixing of Yb 6s and 6p_z as well as Rb(Cs)5p_z (6p_z) atomic orbitals. σ_3 has more of Rb(Cs)5p_z (6p_z) atomic character with larger admixtures of the other atomic orbitals. The $YbSr^+$ and $YbBa^+$ molecules also have similar discernment in the molecular orbital σ_2. The σ_3 molecular orbital is composed of the alkaline-earth-metal atom and Yb p_z atomic orbitals with small admixtures of the respective s atomic orbitals.

If we make the approximation that these two configurations are all that matter in the calculation of $\mathcal{E}_{\mathrm{eff}}$, we can write the total molecular wave function as

$$|\Psi_{\mathrm{tot}}\rangle=c_1|\Psi_1\rangle+c_2|\Psi_2\rangle, \tag{4}$$

where c_1 and c_2 are the MRCI coefficients. Ideally, $c_1^2+c_2^2$ would be unity. However, since other configurations also contribute, the sum $c_1^2+c_2^2$ is approximately 0.95 in all the cases considered.

The total s and p contribution from one of the atoms is given by the weighted sum (weighted by the MRCI coefficients) of the individual s- and p-atomic orbitals as follows:

TABLE IV. Effective electric field estimates for YbRb, YbCs, $YbSr^+$, and $YbBa^+$ in GV/cm. Also presented are the molecular electric-dipole moments (Debye) and the critical field for polarizing the molecules (kV/cm).

Molecule	$\mathcal{E}_{\text{eff}}$	$\mathcal{E}_{\text{eff}}$ (A)	$\mathcal{E}_{\text{eff}}$ (Yb)	d_{m}	$\mathcal{E}_{\text{pol}}$
YbRb $X\ ^2\Sigma$	−0.70	0.45	−1.15	0.21	5.5
YbCs $X\ ^2\Sigma$	0.54	1.42	−0.88	0.24	3.5
$YbSr^+$ $X\ ^2\Sigma$	−11.3	10.6	−21.9	5.1	0.38
$YbBa^+$ $X\ ^2\Sigma$	1.2	12.6	−11.4	5.1	0.25

$$|\psi_{\text{A,s}}\rangle = c_1 \sum_{j=1}^{k} \alpha_j g_j + c_2 \sum_{j=1}^{k} \beta_j g_j. \tag{5}$$

In the above g_j is a Gaussian centered on atom A having s-wave characteristics. The coefficients α_j and β_j describe the relative contributions of each Gaussian g_j to the molecular orbital. c_1 and c_2 are the same MRCI coefficients from the molecular-orbital calculation. We can now define the $\epsilon_{s,\text{A}}$ from atom A as [15,29]

$$\epsilon_{s,\text{A}} = \frac{\langle \psi_{\text{A,s}} | \Psi_{\text{tot}} \rangle}{\langle \psi_{\text{A,s}} | \psi_{\text{A,s}} \rangle}. \tag{6}$$

Similar definitions describe $\epsilon_{\text{p,A}}$, $\epsilon_{\text{s,Yb}}$, and $\epsilon_{\text{p,Yb}}$. The results of the calculation are presented in Table IV.

In Table IV, we have separated out the contributions from both atoms individually. It is apparent that both atoms contribute to the size of the effective electric field, but with the opposite sign. We interpret this as both atoms polarizing in different directions with respect to the molecular axis. Indeed, this is what is observed when one looks at the electronic distribution of the unpaired electron. We also note that $\mathcal{E}_{\text{eff}}$ of the YbRb and YbCs systems makes them an attractive alternative to experiments on the solitary alkali-metal atoms. Even though $\mathcal{E}_{\text{eff}}$ is small compared to other $X\ ^2\Sigma$ molecules, the expected long coherence times in an ultracold sample still makes them appealing. For the lone electron in Rb (Cs) atomic electron EDM experiments, one would have to apply an electric field $\mathcal{E}_{\text{app}}$ of 27 MV/cm (4.5 MV/cm)—using the enhancement factors in [6]—to achieve the same $\mathcal{E}_{\text{eff}}$. This is to be contrasted with the proposed alkali-metal-atom–Yb molecular electron EDM experiment where one needs $\mathcal{E}_{\text{app}} \approx 10-25$ kV/cm. The values of $\mathcal{E}_{\text{app}}$ in the molecular cases are based on multiplying $\mathcal{E}_{\text{pol}}$ by 3–5 in order to be in the linear Stark regime. $\mathcal{E}_{\text{pol}}$ is defined as the electric field required to equalize the Stark energy and the energy splitting between rotational levels in the molecule. $\mathcal{E}_{\text{pol}}$ is tabulated in Table IV.

We have used the following convention for the overall sign of $\mathcal{E}_{\text{eff}}$: we define the molecular axis $\hat{n}$ as pointing from Yb to A, where A is either an alkali-metal or alkaline-earth-metal atom. This is because we choose the axis to point from more negative charge to more positive. In the alkali-metal-atom–Yb molecules, Yb has negative charge while in the alkaline-earth-metal-atom–Yb molecules it has less positive charge. A positive value of $\mathcal{E}_{\text{eff}}$ means that it lies against the direction of $\hat{n}$, i.e., points from positive charge toward negative charge. Positive $\mathcal{E}_{\text{eff}}$, in turn, means that the atomic electron is polarized so that it is displaced in the direction $-\hat{n}$.

These molecules offer alternatives to performing the experiments on Rb and Cs or Sr^+ and Ba^+ alone. In the atoms, the size of $\mathcal{E}_{\text{eff}}$ is proportional to the applied field $\mathcal{E}_{\text{app}}$ by an enhancement factor [4]. In molecules, this is not the case provided they are fully polarized. However, polarizing these molecules is not as easy to do as in the case of $^3\Delta_1$ molecules discussed in [15,29]. Yet, the $\mathcal{E}_{\text{eff}}$ that can be attained is larger than the $\mathcal{E}_{\text{eff}}$ that can be attained in the atomic systems for a similar $\mathcal{E}_{\text{app}}$ [4]. Therefore, with the recent advances in producing cold molecules, these systems offer very intriguing and viable alternative routes to probe for the electron EDM.

Further, various other laser-cooled atoms could be paired with Yb to make useful molecular candidates in an electron EDM search. We chose heavier pairing partners in the hope of reducing the rotational constant of the molecules, thereby, making them easier to polarize in modest applied electric fields. However, as one increases the mass of the pairing partner, one also increases the contribution it gives to $\mathcal{E}_{\text{eff}}$ and this contribution is always opposite to Yb's contribution, thereby, reducing the effect. Therefore, there should be some trade off between reduced rotational constant and overall $\mathcal{E}_{\text{eff}}$. Future work would include exploring systems such as YbK, YbNa, $YbCa^+$, and $YbMg^+$. In addition, the same ideas would work for Hg-paired partners. Work on HgH [30] has already been performed in regard to an electron EDM experiment. Systems such as HgLi, HgNa, etc., should also give similar results as the Yb-paired systems with the added benefit that Hg is heavier than Yb, thereby, hopefully producing a larger $\mathcal{E}_{\text{eff}}$.

V. CONCLUSIONS

We have considered a particular class of $^2\Sigma$ molecules that offer some advantages and drawbacks to current polar molecule electron EDM searches. This type of molecule is formed from ultracold atoms so that the ground-state molecules are also ultracold, leading to the possibility of longer coherence times. We have considered YbRb(−0.7 GV/cm), YbCs(+0.54 GV/cm), $YbSr^+$ (−11.3 GV/cm), and $YbBa^+$ (+1.2 GV/cm).

YbRb and YbCs can be polarized in fairly modest fields and thereby are intriguing inasmuch as they offer some incentive over searching for the electron EDM in the alkali-metal atom alone. The molecular ions $YbSr^+$ and $YbBa^+$

have many useful attributes; however, the field required to polarize these molecules is rather large for an ion trap. Thus, the use of an optical lattice may be more practical for holding these ions for a long period of time without having to rotate an $\mathcal{E}_{\text{app}}$ on the order of 1 kV/cm.

ACKNOWLEDGMENTS

We wish to acknowledge D. DeMille for bringing Yb-containing molecules to our attention, an anonymous referee for a crucial observation, and the NSF for financial support.

[1] J. J. Hudson, B. E. Sauer, M. R. Tarbutt, and E. A. Hinds, Phys. Rev. Lett. **89**, 023003 (2002).
[2] N. E. Shafer-Ray, Phys. Rev. A **73**, 034102 (2006).
[3] W. Bernreuther and M. Suzuki, Rev. Mod. Phys. **63**, 313 (1991).
[4] I. B. Khriplovich and S. K. Lamoreaux, *CP Violation Without Strangeness* (Springer-Verlag, Berlin, 1997).
[5] H. S. Nataraj, B. K. Sahoo, B. P. Das, and D. Mukherjee, Phys. Rev. Lett. **101**, 033002 (2008).
[6] D. S. Weiss, F. Fang, and J. Chen, Bull. Am. Phys. Soc. **48**, J1008 (2003).
[7] J. M. Amini, Jr., C. T. Munger, and H. Gould, Phys. Rev. A **75**, 063416 (2007).
[8] P. G. Sandars and E. Lipworth, Phys. Rev. Lett. **13**, 718 (1964).
[9] M. G. Kozlov, A. V. Titov, N. S. Mosyagin, and P. V. Souchko, Phys. Rev. A **56**, R3326 (1997).
[10] Y. Takasu, K. Honda, K. Komori, T. Kuwamoto, M. Kumakura, Y. Takahashi, and T. Yabuzaki, Phys. Rev. Lett. **90**, 023003 (2003).
[11] S. De, U. Dammalapati, K. Jungmann, and L. Willmann, Phys. Rev. A **79**, 041402(R) (2009).
[12] X. Y. Xu *et al.*, J. Opt. Soc. Am. B **20**, 968 (2003).
[13] N. Nemitz, F. Baumer, F. Münchow, S. Tassy, and A. Gorlitz, Phys. Rev. A **79**, 061403(R) (2009).
[14] M. G. Kozlov and V. V. Yashchuk, Sov. Phys. JETP **64**, 709 (1996).
[15] E. R. Meyer and J. L. Bohn, Phys. Rev. A **78**, 010502(R) (2008).
[16] H. J. Metcalf and P. van der Straten, *Laser Cooling and Trapping* (Springer-Verlag, Berlin, 1999).
[17] H. J. Werner *et al.*, MOLPRO, version 2008.1, a package of *ab initio* programs (2003); see http://www.molpro.net
[18] H.-J. Werner and P. J. Knowles, J. Chem. Phys. **82**, 5053 (1985).
[19] P. J. Knowles and H.-J. Werner, Chem. Phys. Lett. **115**, 259 (1985).
[20] H.-J. Werner and P. J. Knowles, J. Chem. Phys. **89**, 5803 (1988).
[21] P. J. Knowles and H.-J. Werner, Chem. Phys. Lett. **145**, 514 (1988).
[22] Y. Wang and M. Dolg, Theor. Chem. Acc. **100**, 124 (1998).
[23] L. von Szentpaly, P. Fuentealba, H. Preuss, and H. Stoll, Chem. Phys. Lett. **93**, 555 (1982).
[24] P. Fuentealba, H. Stoll, L. v. Szentpaly, P. Schwerdtfeger, and H. Preuss, J. Phys. B **16**, L323 (1983).
[25] K.-K. Ni, S. Ospelkaus, A. Pe'er, M. H. G. de Miranda, B. Neyenhuis, J. J. Zirbel, S. Kotochigova, P. S. Julienne, D. S. Jin, and J. Ye, Science **322**, 231 (2008).
[26] E. R. Hudson, N. B. Gilfoy, S. Kotochigova, J. M. Sage, and D. DeMille, Phys. Rev. Lett. **100**, 203201 (2008).
[27] J. G. Danzl *et al.*, Faraday Discuss. **142**, 283 (2009).
[28] R. Stutz and E. A. Cornell, Bull. Am. Phys. Soc. **89**, 76 (2004).
[29] E. R. Meyer, J. L. Bohn, and M. P. Deskevich, Phys. Rev. A **73**, 062108 (2006).
[30] M. G. Kozlov and A. Derevianko, Phys. Rev. Lett. **97**, 063001 (2006).